

Dynamic Characterization of Distortion in Hybrid Silicon Evanescent Phase Modulators

Nobuhiro Nunoya, *Member, IEEE*, Anand Ramaswamy, *Student Member, IEEE*, Hui-Wen Chen, *Student Member, IEEE*, Matthew N. Sysak, *Member, IEEE*, and John E. Bowers, *Fellow, IEEE*

Abstract—We report the dynamic distortion of hybrid silicon phase modulators for three types of active layers. The third-order intermodulation distortion for each modulator was measured under various bias conditions by means of a two-tone technique. A peak phase input intercept point of 2.6π for doped quantum-well modulators was achieved at a reverse bias of 4 V and a signal frequency of around 500 MHz.

Index Terms—Carrier depletion, phase modulators, quantum confined Stark effect (QCSE), silicon-on-insulator technology.

I. INTRODUCTION

LINEAR phase modulators are key components in both digital and analog communication systems that employ phase modulation because they can provide increased receiver sensitivity and improved tolerance to fiber dispersion [1]. To characterize the linearity of phase modulators, several techniques have been reported [2], [4]. One such technique involves measuring resonance peak shifts in Fabry–Pérot cavities to determine refractive index shift (i.e., phase shift) as a function of applied dc bias [2]. Another way is to convert the phase shift to an intensity variation by utilizing a Mach–Zehnder interferometer (MZI). However, it cannot be extended to higher frequencies because the phase detection process using an MZI also induces signal distortion via the sinusoidal response of the interferometer [3]. In order to measure only the nonlinearities produced by the phase modulator, Sysak *et al.* reported a two-tone measurement technique that decouples distortion generated in the phase detection process from the distortion of the phase modulator under test [4].

Currently, there is a lot of interest in silicon photonics because of the potential to integrate photonics devices with complementary metal–oxide–semiconductor electronics at low cost. Several optical devices have been demonstrated by utilizing a technique that bonds III–V materials onto silicon waveguides [5], [6]. In this work, we focus on characterizing the linearity of

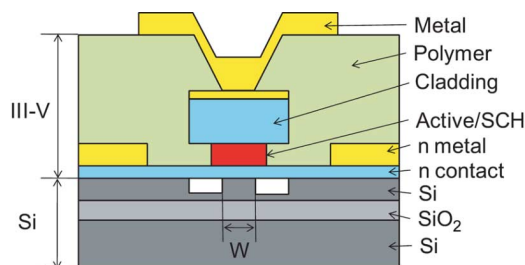


Fig. 1. Schematic view of the hybrid silicon evanescent modulator.

the modulators since they are important components for determining the feasibility of high performance microwave photonic links.

II. DEVICE STRUCTURE AND MEASUREMENT SETUP

A schematic of the cross-sectional structure of the hybrid silicon evanescent modulator is shown in Fig. 1, where III–V material is bonded to fabricated silicon waveguides. The width of the silicon waveguide (W) is $1.5\ \mu\text{m}$, while the length of the hybrid section (L) of the modulator is 1 mm. To investigate the linearity imposed by various physical effects in the active region, three types of III–V active layers are prepared. The layer structures of doped quantum-well (QW), undoped QW, and doped bulk are listed in Tables I, II, and III, respectively. In Tables II and III, only active layers and separate confinement heterostructure (SCH) layers are listed because the other layers are identical to that of the doped QW structure shown in Table I. As can be seen, the doped QW structure consists of lightly doped QW, barriers and top SCH layer while undoped QW has identical structure without any doping. The doped bulk material, on the other hand, has a lattice-matched InAlGaAs active region with the same amount of doping. The waveguide in the III–V material is oriented along the $\langle 01\bar{1} \rangle$ direction. The physical dimensions of the devices are the same for all three types of modulators. More details about the modulator structure and fabrication process can be found in [6].

Fig. 2 shows the measurement system to determine the third-order intermodulation distortion (IMD3) contribution of a phase modulator, that is, the intercept point (IP3) of the fundamental signals (f_1, f_2) and IMD3 signals ($2f_1 - f_2, 2f_2 - f_1$) [4]. Dashed lines represent optical paths and solid lines indicate electrical paths. Light from a 1550-nm source is split into the two arms of an MZI by a polarizing beam splitter, in which the splitting ratio can be changed by means of the polarization controller. In the upper arm of the interferometer, it can be seen that the electrical signal from two microwave synthesizers is combined and then split before being applied to a LiNbO₃ reference phase modulator (PM1) and the hybrid silicon phase modulator

Manuscript received December 15, 2008; revised March 10, 2009. First published April 10, 2009; current version published June 10, 2009. This work was supported by the Defense Advanced Research Projects Agency (DARPA) PHOR-FRONT program under U.S. Air Force Contract FA8750-05-C-0265.

N. Nunoya, A. Ramaswamy, H.-W. Chen, and J. E. Bowers are with the Department of Electrical and Computer Engineering, University of California, Santa Barbara, CA 93106 USA (e-mail: nunoya@ece.ucsb.edu; nunoya@aecl.ntt.co.jp; anand@ece.ucsb.edu; hwchen@ece.ucsb.edu; bowers@ece.ucsb.edu).

M. N. Sysak is with the Department of Electrical and Computer Engineering, University of California, Santa Barbara, CA 93106 USA, and also with Intel Corporation, Santa Clara, CA 95054 USA (e-mail: matthew.n.sysak@intel.com).

Color versions of one or more of the figures in this letter are available online at <http://ieeexplore.ieee.org>.

Digital Object Identifier 10.1109/LPT.2009.2019623

TABLE I
LAYER STRUCTURE OF DOPED QW

Layer	Material and Composition	Doping	Thickness
p Contact	In _{0.53} Ga _{0.47} As	p-1e19	0.1 μm
Cladding	InP	p-1e18	1.5 μm
SCH	In _{0.53} Al _{0.165} Ga _{0.305} As, 1.3 μm	n-1e17	0.1 μm
QW	In _{0.574} Al _{0.111} Ga _{0.315} As,+0.3%(15x)	n-1e17	8 nm
(λ _{PL} =1.36 μm)	In _{0.468} Al _{0.217} Ga _{0.315} As,-0.41%(16x)	n-1e17	5 nm
SCH	In _{0.53} Al _{0.165} Ga _{0.305} As, 1.3 μm	n-3e18	0.05 μm
n Contact	InP	n-3e18	0.11 μm
Super lattice	In _{0.85} Ga _{0.15} As _{0.327} P _{0.673} (2x)	n-3e18	7.5 nm
	InP (2x)	n-3e18	7.5 nm
Bonding	InP	n-3e18	10 nm

TABLE II
LAYER STRUCTURE OF UNDOPED QW

Layer	Material and Composition	Doping	Thickness
SCH	In _{0.53} Al _{0.165} Ga _{0.305} As, 1.3 μm	i	0.1 μm
QW	In _{0.574} Al _{0.111} Ga _{0.315} As,+0.3%(15x)	i	8 nm
(λ _{PL} =1.36 μm)	In _{0.468} Al _{0.217} Ga _{0.315} As,-0.41%(16x)	i	5 nm
SCH	In _{0.53} Al _{0.165} Ga _{0.305} As, 1.3 μm	n-3e18	0.05 μm

TABLE III
LAYER STRUCTURE OF DOPED BULK

Layer	Material and Composition	Doping	Thickness
SCH	In _{0.53} Al _{0.165} Ga _{0.305} As, 1.3 μm	n-1e17	0.1 μm
Active	In _{0.53} Al _{0.151} Ga _{0.319} As, 1.33 μm	n-1e17	0.2 μm
SCH	In _{0.53} Al _{0.165} Ga _{0.305} As, 1.3 μm	n-3e18	0.05 μm

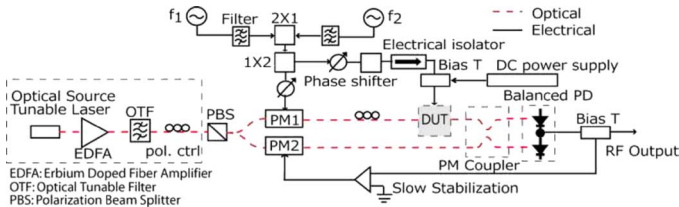


Fig. 2. Measurement setup for the characterization of the dynamic distortions in the phase modulator. Optical paths and electrical paths are indicated as dashed lines and solid lines, respectively.

device under test (DUT). The signal frequencies are 504.9 MHz for f_1 and 505.1 MHz for f_2 . The variable attenuators in the electrical path ensure that the drive signal to the two modulators produces the same phase swing in each device. Additionally, the electrical path length between the 1 : 2 splitter and the DUT is adjusted to achieve a phase delay of π radians. The phase modulator (PM2) in the lower arm of the MZI forms part of a slow feedback circuit that is used to stabilize the MZI about the quadrature point. At the output of the interferometer, the two light waves are combined, and the interfered signals are detected using a balanced photodiodes (PDs) made with linear (Output IP3 = 20 dBm) commercial detectors for the community antenna television (CATV).

Theoretically, the phase detection process causes distortion with a peak phase IP3 of 0.9π due to the sinusoidal response of MZI [3]. However, since equal phase swing is applied to both PM1 and the DUT, the fundamental signals can be cancelled significantly because of the π phase delay [4]. Consequently, this results in suppression of IMD3 due to the sinusoidal response of

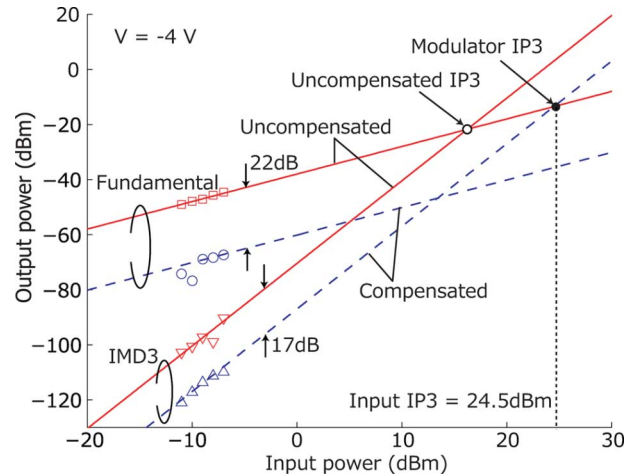


Fig. 3. Uncompensated and compensated experimental results for the doped QW modulator at a reverse bias of 4 V.

the MZI. It is important to note that the IMD3 generated in the DUT is not cancelled because of the significantly more linear response of the commercial LiNbO₃ reference modulator in which the linear electrooptic effect is dominant [7]. Hence, the residual distortion that is measured can be attributed to the DUT.

III. RESULTS AND DISCUSSION

Fig. 3 shows the measurement results of doped QW modulator for a reverse bias of 4 V. An uncompensated measurement of the DUT was taken without PM1 to determine the fundamental output intensity and IMD3 signals including distortion due to the phase detection process. In a compensated measurement using both DUT and PM1, fundamental signals were cancelled by 22 dB. This would translate into a 66-dB reduction of IMD3 due to the system. However, the IMD3 drops only by 17 dB indicating that this distortion is caused by the DUT. The IP3 of the modulator is defined by the intersection point of uncompensated fundamental signals and compensated IMD3 signals. An uncompensated input IP3 of 16.2 dBm and a modulator input IP3 of 24.5 dBm were obtained. Since the semiconductor phase modulator also has some residual amplitude modulation, it will add some error to the measured linearity thru the phase detection process. There is about 2% fluctuation of optical output power with a 0.1-V voltage swing in our modulators.

A π phase shift voltage ($V_{\pi,RF}$) of the modulator under a dc reverse bias voltage of 4 V was 2.1 V. It was estimated from the difference of input powers between the DUT and PM1 to cancel the fundamental frequency component at 505.1 MHz, where the V_{π} of PM1 is 5.5 V. Using this experimentally determined $V_{\pi,RF}$, a peak phase input IP3 (IIP3) for uncompensated IP3 is calculated to be 0.99π . This is in close agreement with the theoretically predicted peak phase IP3 of 0.9π coming from the MZI. Therefore, the measurement system consisting of the MZI works as expected. To confirm the $V_{\pi,RF}$ value calculated from the difference of applied input signal powers to PM1 and DUT, dynamic $V_{\pi,RF}$ measurements were carried out. The response of the phase demodulation process utilizing an MZI and a balanced PD is sinusoidal as shown in Fig. 4. By removing PM1 in Fig. 2 and increasing the power of the input signal to the DUT, distortion of the output signal increases and the response of the interferometer changes from being purely sinusoidal. When the

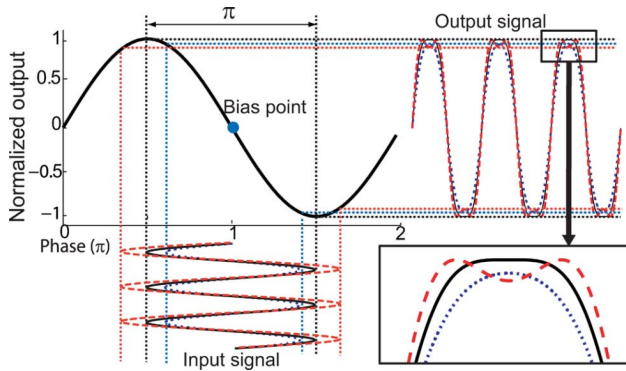


Fig. 4. Dynamic V_{π} measurement of phase modulators by utilizing measurement setup shown in Fig. 2.

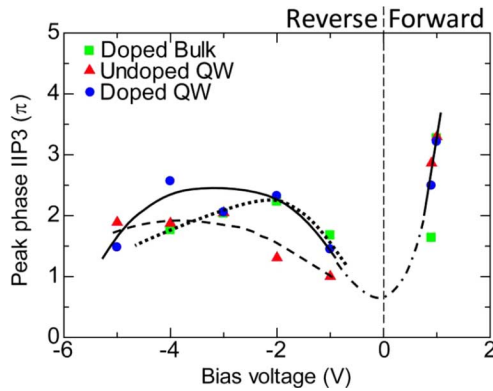


Fig. 5. Bias voltage dependence of peak phase input IP3 for three types of modulators.

applied RF signal results in close to π phase swing in the DUT, a double peak is observed as shown in the inset in Fig. 4. By measuring the peak-to-peak voltage in an oscilloscope, the $V_{\pi,RF}$ was determined to be 2.0 V, which is almost identical to the calculated value based on the difference of input powers to the DUT and PM1. Using this technique, we also confirmed the V_{π} of PM1 to be around 5.5 V.

Fig. 5 shows the bias voltage dependence of peak phase IIP3 for three kinds of modulators. Under reverse bias, a solid line, a dashed line, and a dotted line show the trends of peak phase IIP3 for doped QW, undoped QW, and doped bulk, respectively. The major effects to introduce index change in such material systems can be divided into carrier effects [plasma and band-filling (BF)] and electrical field effects [Pockels, Kerr, and quantum confined Stark effects (QCSE)]. In [4], a peak phase IIP3 of 0.97π was reported for GaInAsP–InP undoped QW modulator at a bias of -2 V, which is close to the results of the undoped QW at -2 V (1.3π) in this measurement. In terms of linearity, both doped structures (both QW and bulk) are better than undoped QW under low bias conditions, because undoped QW has higher QCSE which results in a more nonlinear index shift in response to an applied electrical field [8]. In contrast, the index change of the doped structures is dominated by carrier effects, and QCSE is relatively weak at low reverse bias voltages because the applied electric field drops predominantly across the SCH region. Additionally, carriers presented in the QW region could further reduce the QCSE by changing the electric field profile. As the bias voltage increases to higher region, the car-

rier effects become saturated and hence result in nonlinear index shift. The doped QW, however, different from doped bulk material, has more obvious QCSE at higher bias since the electrical field across the active region is stronger. This QCSE balances with the reduction in linearity due to the saturation of carrier depletion effects, thus the combination of these two effects inside doped QW keeps the linearity high. However, at a bias over -5 V, not only QCSE but also space charge effect due to absorbed carriers degrades overall linearity. And also, the doped QW is effective in high-speed operation [9].

For the forward bias, peak phase IIP3s are much better than those of reverse bias for all kinds of modulators because even a small injection of carriers changes the refractive index greatly. Within the vicinity of a certain forward bias, the index change and consequent phase shift can be very linear. We obtained a phase peak IIP3 of around 3.2π at a forward bias of 2 V for doped QW, of which V_{π} was 0.92 V. However, for even higher frequency operation, forward biasing the modulator may not be suitable because carrier injection effects tend to be slower [10].

IV. CONCLUSION

The linearity of silicon evanescent modulators with different active regions structures is measured dynamically at a signal frequency of ~ 500 MHz. A peak phase IIP3 of 2.6π was achieved for the doped QW modulator at a reverse bias of -4 V, which is better than that of the undoped QW reported here.

ACKNOWLEDGMENT

The authors would like to thank, L. A. Johansson and S. Ristic for useful discussions and M. Piels for assisting with measurements.

REFERENCES

- [1] R. F. Kalman, J. C. Fan, and L. G. Kazovsky, "Dynamic range of coherent analog fiber-optic links," *J. Lightw. Technol.*, vol. 12, no. 7, pp. 1263–1277, Jul. 1994.
- [2] H. Mohseni, H. An, Z. A. Shellenbarger, M. H. Kwakernaak, and J. H. Abeles, "Highly linear and efficient phase modulators based on GaInAsP–InP three step quantum wells," *Appl. Phys. Lett.*, vol. 86, p. 031103, 2005.
- [3] B. Kolner and D. W. Dolfi, "Intermodulation distortion and compression in an integrated electrooptic modulator," *Appl. Opt.*, vol. 26, no. 17, pp. 3676–3680, Sep. 1987.
- [4] M. N. Sysak, L. Johansson, J. Klamkin, L. A. Coldren, and J. E. Bowers, "A dynamic measurement technique for third-order distortion in optical phase modulators," *IEEE Photon. Technol. Lett.*, vol. 19, no. 3, pp. 170–172, Feb. 1, 2007.
- [5] A. W. Fang, B. R. Kock, R. Jones, E. Lively, D. Liang, Y.-H. Kuo, and J. E. Bowers, "A distributed bragg reflector silicon evanescent laser," *IEEE Photon. Technol. Lett.*, vol. 20, no. 20, pp. 1667–1669, Oct. 15, 2008.
- [6] H.-W. Chen, Y.-H. Kuo, and J. E. Bowers, "A hybrid silicon–Al–GaInAs phase modulator," *IEEE Photon. Technol. Lett.*, vol. 20, no. 23, pp. 1920–1922, Dec. 1, 2008.
- [7] A. Yariv and P. Yeh, *Optical Waves in Crystals*. New York: Wiley, 1984, ch. 7, pp. 220–238.
- [8] W. Bardyszewski, D. Yevick, Y. Liu, C. Rolland, and S. Bradshaw, "Theoretical and experimental analysis of Mach–Zehnder quantum-well modulators," *J. Appl. Phys.*, vol. 80, no. 2, pp. 1136–1141, Jul. 1996.
- [9] H.-W. Chen, Y.-H. Kuo, and J. E. Bowers, "High speed hybrid silicon evanescent Mach–Zehnder modulator and switch," *Opt. Express*, vol. 16, no. 25, pp. 20571–20576, Dec. 2008.
- [10] O. Mikami and H. Nakagome, "Waveguided optical switch in In–GaAs/InP using free-carrier plasma dispersion," *Electron. Lett.*, vol. 20, pp. 228–229, Mar. 1984.